



Published in final edited form as:

*Biochemistry*. 2013 September 24; 52(38): . doi:10.1021/bi4009984.

## DEER EPR Measurements for Membrane Protein Structures via Bi-functional Spin Labels and Lipodisq Nanoparticles

Indra D. Sahu<sup>1</sup>, Robert M. McCarrick<sup>1</sup>, Kaylee R. Troxel<sup>1</sup>, Rongfu Zhang<sup>1</sup>, Hubbell J. Smith<sup>1</sup>, Megan M. Dunagan<sup>1</sup>, Max S. Swartz<sup>1</sup>, Prashant V. Rajan<sup>1</sup>, Brett Kroncke<sup>2</sup>, Charles R. Sanders<sup>2</sup>, and Gary A. Lorigan<sup>1,\*</sup>

<sup>1</sup>Department of Chemistry and Biochemistry, Miami University, Oxford, Ohio 45056

<sup>2</sup>Department of Biochemistry and Center for Structural Biology, Vanderbilt University, Nashville, Tennessee 37232

### Abstract

Pulsed EPR DEER structural studies of membrane proteins in a lipid bilayer have often been hindered by difficulties in extracting accurate distances when compared to globular proteins. In this study, we employed a combination of three recently developed methodologies: 1) bi-functional spin labels (BSL), 2) SMA-Lipodisq nanoparticles, and 3) Q-band pulsed EPR measurements to obtain improved signal sensitivity, increased transverse relaxation time, and more accurate and precise distances in DEER measurements on the integral membrane protein KCNE1. The KCNE1 EPR data indicated ~2 fold increase in the transverse relaxation time for the SMA-Lipodisq nanoparticles when compared to proteoliposomes, and narrower distance distributions for the BSL when compared to the standard MTSL. The certainty of information content in DEER data obtained for KCNE1 in SMA-Lipodisq nanoparticles is comparable to that in micelles. The combination of techniques will enable researchers to potentially obtain more precise distances in cases where the traditional spin labels and membrane systems yield imprecise distance distributions.

### Keywords

Membrane protein; DEER spectroscopy; Spin labeling; Proteoliposomes; Lipodisq nanoparticles; KCNE1

## INTRODUCTION

Pulsed electron double resonance (PELDOR)/double electron-electron resonance (DEER) EPR spectroscopy, in combination with site-directed spin labeling, is a powerful structural biology technique used to obtain long range distances of ~20-80 Å by measuring the dipolar coupling between two unpaired electron spins.<sup>1,2</sup> These distance measurements provide valuable structural information from systems in which other techniques like solution NMR or X-ray crystallography prove difficult or impossible.<sup>3,4</sup> However, the application of DEER spectroscopy to study membrane proteins can still be difficult due to much shorter

\*Corresponding Author: gary.lorigan@miamioh.edu. Phone: (513) 529-3338 .

### Notes

The authors declare no competing financial interest.

### Supporting Information

Table S1, and Figures S1, S2 and S3. This material is available free of charge via the Internet at <http://pubs.acs.org>

transverse relaxation times ( $T_2$ ) or phase memory times ( $T_m$ ) and poor DEER modulation in more biologically relevant proteoliposomes as compared to water soluble proteins or membrane proteins in detergent micelles. Frequently membrane protein DEER experiments are conducted with spin labels located outside the membrane to specifically avoid these challenging problems. The combination of these factors often leads to broad distance distributions, poorer signal to noise, and limitations in the determination of longer distances. The short phase memory times are typically due to uneven distributions of the spin labeled protein within the membrane, which creates local inhomogeneous pockets of high spin concentrations.<sup>4</sup> Some useful techniques used to minimize these limitations include the use of low protein/lipid molar ratio, and reconstitutions in the presence of unlabeled proteins, bicelles, nanodiscs, and lipodisc nanoparticles.<sup>5-9</sup> To compliment other promising approaches that have recently been introduced to optimize the sample conditions for DEER spectroscopy on membrane proteins,<sup>6-11</sup> this study introduces the combination of three recently developed methodologies: bi-functional spin labels (BSL),<sup>12</sup> lipodisc nanoparticles sample preparation<sup>13</sup> and Q-band pulsed EPR measurements.<sup>8, 14-16</sup> These approaches increase phase memory times ( $T_m$ ) and signal sensitivity to achieve higher quality DEER distance measurements.

Bi-functional spin labels can be introduced by a facile cross linking reaction of a bi-functional methanethiosulfonate reagent with pairs of cysteine residues at  $i$  and  $i + 3$  or  $i$  and  $i + 4$  in an helix, at  $i$  and  $i + 1$  or  $i + 2$  in a strand.<sup>12</sup> These spin labels are rigid and thus very useful for obtaining tighter DEER distance distributions when compared to traditional mobile MTSL.<sup>12</sup> However, DEER studies incorporating the unique BSL have not been published on a membrane protein system.

Membrane scaffold protein (MSP)-stabilized nanodiscs are a very promising approach to facilitate the formation of monodispersed protein samples under bilayer conditions to minimize the detrimental effect of pockets of high local electron spin concentrations on the transverse relaxation within a sample.<sup>8</sup> However, there are drawbacks to this method in that it requires the use of detergents for protein incorporation which must then be completely removed for the assembly of a protein-nanodisc complex.<sup>17</sup> In addition, the absorbance properties of the membrane scaffold protein may interfere with the incorporated protein of interest introducing uncertainty in the concentration measurement or there may be specific lipid interactions with the rim protein. In this work, we incorporated a BSL-KCNE1 liposome complex into SMA-Lipodisc nanoparticles.<sup>13, 17</sup> Lipodisc nanoparticles are lipid-polymer complexes that are easily formed by detergent-free methods from a range of different lipid compositions. The polymer does not have the same interfering absorbance properties that nanodisc rim proteins possess.<sup>17</sup> SMA-Lipodisc nanoparticles isolate protein macromolecules by minimizing the size of the complex to ~10-15 nm while still retaining a biologically relevant membrane structure.<sup>13</sup>

DEER experiments have historically been carried out at X-band (~9.5 GHz). However, the trend is now moving towards Q-band to increase sensitivity. X-band DEER experiments can suffer from poor signal to noise and extended data collection times. This, coupled with low  $T_m$  values can make the use of X-band DEER for membrane protein systems extremely challenging. Our lab and others have previously reported an increase in sensitivity in DEER measurements for proteins or peptides when the experiment is performed at Q-band when compared to X-band.<sup>8, 14-16</sup> The use of Q-band DEER spectroscopy coupled with the methods detailed above has yielded very high quality data on a membrane protein system which has proven difficult using more traditional structural biology techniques.

KCNE1 is a single transmembrane protein consisting of 129 amino acids that modulates the function of certain voltage gated potassium ion channels ( $K_v$ ).<sup>18-20</sup> Recent biochemical and

electrophysiological studies indicated that the transmembrane domain (TMD) of KCNE1 binds to the pore domain of the KCNQ1 channel modulating the channel's gating.<sup>21-24</sup> Mutations in the genes encoding these proteins result in increased susceptibility to genetic diseases such as congenital deafness, congenital long QT syndrome, ventricular tachyarrhythmia, syncope, and sudden cardiac death.<sup>19, 25, 26</sup> The combination of the techniques used in this study was applied to KCNE1 and found to give superior DEER results.

## MATERIALS AND METHODS

### Site-directed mutagenesis

The His-tag expression vectors (pET-16b) containing a cysteine-less mutant of KCNE1 were transformed into XL1-Blue *Escherichia coli* cells (Stratagene). Plasmid extracts from these cells were obtained using the QIAprep spin miniprep kit (Qiagen). Site-directed cysteine mutants were introduced into the cysteine-less KCNE1 gene using the Quickchange lightning site-directed mutagenesis kit (Stratagene). The KCNE1 mutations were confirmed by DNA sequencing<sup>12</sup> from XL10-Gold *E. coli* (Stratagene) transformants using the T7 primer (Integrated DNA Technologies). Successfully mutated vectors were transformed into BL21-(DE3) CodonPlus-RP *E. coli* cells (Stratagene) for protein over expression. Double BSL mutants (Tyr46-Val50/Ile66-Lys70) were generated by introducing two pairs of Cys residues at the i and i+4 positions (46, 50, 66 and 70). Double MTSL mutants (Val47/Ile66) were generated by introducing a pair of cysteines at 47 and 66 positions. All spin labeling sites are located inside the membrane.<sup>20</sup>

### Expression and Purification of KCNE1

The over expression and purification of *E. coli* BL21 cells carrying mutated KCNE1 genes were carried out using a previously described protocol.<sup>20</sup> *E. coli* cells carrying mutants of choice were grown in an M9 minimal medium with 50 µg/mL ampicillin. The cell culture was incubated at 37 °C and 240 rpm until the OD<sub>600</sub> reached 0.8, at which point protein expression was induced using 1 mM IPTG (isopropyl-1-thio-D-galactopyranoside), followed by continued rotary shaking at 37°C for 16 h. Purification of KCNE1 from inclusion bodies was carried out according to a previous method,<sup>19</sup> with final elution of pure protein into 0.05% LMPG or 0.2% SDS detergent (buffer: 250 mM IMD, 200mM NaCl, 20 mM Tris, pH 7.8). Protein samples were concentrated to 1mL by using a 3.5 kDa molecular mass cutoff spin column (Millipore). Protein concentration was determined from the A280 using an extinction coefficient of 1.2 mg/mL per 1.0 absorbance on a NanoDrop 200c (Thermo Scientific). The protein purity from over-expression was confirmed by sodium dodecyl sulfate polyacrylamide gel electrophoresis (SDS-PAGE).

### Spin Labeling and Reconstitution into Proteoliposomes

The bi-functional spin label (BSL) (3,4-Bis-(methanethiosulfonylmethyl)-2,2,5,5-tetramethyl 2,5-dihydro-1H-pyrrol-1-yloxy Radical) (HO-1944) and 1 oxyl 2,2,5,5-tetramethylpyrroline-3-methylmethanethiosulfonate (MTSL) spin label were obtained from Toronto Research Chemicals Inc., Toronto, Canada. The spin labels were dissolved in methanol to a concentration of 250 mM and added directly to the concentrated protein in elution buffer at a 10:1 spin label:protein molar ratio and then reacted for 24 hours with gentle shaking at room temperature in the dark to complete labeling. Excess/unreacted free spin labels were removed by extensive dialysis. Dialysis was carried out at room temperature in a regenerated cellulose dialysis tubing (Fisher brand MW cutoff 3.5 kDa) against 1L dialysis buffer (100 mM NaH<sub>2</sub>PO<sub>4</sub>, pH 7.8) and 0.2% SDS without reducing agent for a week with buffer changes twice daily. The spin labeling efficiency was determined by comparing the nano-drop UV A280 protein concentration with spin

concentration obtained from CW EPR spectroscopy. The protein concentration for all KCNE1 samples was ~ 75  $\mu\text{M}$ , and the spin labeling efficiency for all samples was ~ 75 %.

The reconstitution of spin labeled protein into POPC/POPG (3:1) proteoliposomes was carried out via standard dialysis methods following a similar protocol in the literature.<sup>27</sup> The concentrated spin labeled KCNE1 protein was mixed with a stock lipid slurry (400 mM SDS, 75 mM POPC and 25 mM POPG, 0.1 mM EDTA, 100mM IMD, pH 6.5). The lipid slurry had been mixed to generate optically clear mixed micelles via extensive freeze thaw cycles. The final protein:lipid molar ratio was set to 1:400. The KCNE1-lipid mixture was then subjected to extensive dialysis to remove all SDS present, during which KCNE1/POPC/POPG vesicles spontaneously formed. The 4 L dialysis buffer (10 mM imidazole and 0.1 mM EDTA at pH 6.5) was changed two times daily. The completion of SDS removal was determined when the KCNE1-lipid solution became cloudy and the surface tension of the dialysate indicated complete removal of detergent. The KCNE1-lipid vesicles solution was then extruded using a 100 nm filter to generate unilamellar vesicles.

### Reconstitution into Lipodisq Nanoparticles

The SMA-lipodisq nanoparticles were obtained from Malvern Cosmeceutics. The protein lipid complex was incorporated into SMA-lipodisq nanoparticles following published protocols.<sup>13, 17</sup> A 500  $\mu\text{l}$  aliquot of proteoliposome-reconstituted protein sample (30 mM POPC/POPG lipid) was added with the same amount (500  $\mu\text{l}$ ) of 2.5% of lipodisq solution prepared in the same dialysis buffer (10 mM Imidazole, 0.1mM EDTA at pH 6.5) dropwise over 3-4 minutes. The protein-lipodisq solution was allowed to equilibrate overnight at 4°C. The resulting solution was centrifuged at 40,000xg for 30 minutes to remove nonsolubilized protein. The size and homogeneity of the final complex was confirmed by dynamic light scattering (DLS) experiments.

### EPR spectroscopic measurements

EPR experiments were conducted at the Ohio Advanced EPR Laboratory. CW-EPR spectra were collected at X-band on a Bruker EMX CW-EPR spectrometer using an ER041xG microwave bridge and ER4119-HS cavity coupled with a BVT 3000 nitrogen gas temperature controller. Each spin-labeled CW-EPR spectrum was acquired by signal averaging 25 42-s field scans with a central field of 3315 G and sweep width of 100 G, modulation frequency of 100 kHz, modulation amplitude of 1 G, and microwave power of 10 mW at 296 K.

Four pulse DEER experiments were performed using a Bruker ELEXSYS E580 spectrometer equipped with a SuperQ-FT pulse Q-band system with a 10 W amplifier and EN5107D2 resonator. All DEER samples were prepared at a spin concentration of 100-120  $\mu\text{M}$ . 30% (w/w) deuterated glycerol was used as a cryoprotectant. The sample was loaded into a 1.1 mm inner diameter quartz capillary (Wilmad LabGlass, Buena, NJ) and mounted into the sample holder (plastic rod) inserted into the resonator. DEER data were collected using the standard four pulse sequence<sup>4</sup>  $[(\pi/2) - \tau - (\pi) - t - (\pi) - 2\tau - (\pi) - \tau - \text{echo}]$  at Q-band with a probe pulse width of 10/20 ns, pump pulse width of 24 ns, 80 MHz of frequency difference between probe and pump pulse, shot repetition time determined by spin-lattice relaxation time ( $T_1$ ), 100 echoes/point, and 2-step phase cycling at 80 K collected out to ~ 2.0  $\mu\text{s}$  for overnight data acquisition time (12 hours).<sup>28</sup> DEER data were analyzed using DEER Analysis 2011.<sup>29</sup> The distance distributions  $P(r)$  were obtained by Tikhonov regularization<sup>30</sup> in the distance domain, incorporating the constraint  $P(r) > 0$ . A homogeneous three-dimensional model for micelle samples and a homogeneous two-dimensional model for proteoliposomes and lipodisq nanoparticles samples were used for background correction. The regularization parameter in the L curve was optimized by

examining the fit of the time domain. Transverse relaxation data were collected by using the standard Hahn echo pulse sequence [( $\pi/2$ )- $\tau$ -( $\pi$ )- $\tau$ -echo] at Q-band with 10/20 ns pulse widths, an initial  $\tau$  of 200 ns and an increment of 16 ns, 100 echoes/point, and 2-step phase cycling at 80K. The transverse relaxation time ( $T_2$ ) or phase memory time ( $T_m$ ) was determined by fitting the data with a single exponential decay.

The signal-to-noise ratio (S/N) was calculated from time domain DEER data of all the samples using a previously described method.<sup>14</sup> S/N was calculated as the ratio of modulation amplitude to the noise level. The noise level was estimated as a root mean square deviation (rmsd) of the background uncorrected experimental data after subtracting the polynomial fit. The optimized degree of polynomial used was 9.<sup>14</sup> Only the flat part of the baseline trace was included in the rmsd calculation.

## RESULTS AND DISCUSSIONS

Figure 1 displays schematic representations of the spin labels used in this study and the solution NMR structure of KCNE1 in LMPG micelles.<sup>18</sup> Figure 2 shows DEER data for MTSL spin-labeled KCNE1 (Val47/Ile66) samples for (A) 1% LMPG micelles, (B) POPC/POPG proteoliposomes, and (C) POPC/POPG lipodisq nanoparticles. Figure 3 shows DEER data for BSL-KCNE1 (Tyr46 Val50/Ile66-Lys70) for (A) 1% LMPG micelles, (B) POPC/POPG proteoliposomes, and (C) POPC/POPG lipodisq nanoparticles. The left panel represents the time domain traces and the right panel reveals the distance distributions for Figures 2 and 3. All of the DEER distances derived from either the maximum peak intensity or the average distance from the entire peak were within an angstrom of 32 Å. This distance agrees well with the KCNE1 LMPG micelle structure.<sup>18</sup> The approximate full width of the distribution at half maxima (FWHM) for both spin labels are summarized in Table 1. Further analysis of DEER data including the Pake pattern, Tikhonov L-curve, and signal to noise ratio (S/N) are provided in the Supporting Information (Table S1 and Figures S1 and S2). The FWHM values, S/N, and quality of Tikhonov L-curve varied significantly for the different data sets depending upon the combination of spin label and membrane protein sample preparation. The signal to noise ratio (S/N) for spin-labeled KCNE1 in lipodisq nanoparticles increased 3 to 4 fold when compared to proteoliposomes (see Table S1) due to an increase in the phase memory time ( $T_m$ ). The  $T_m$  curves for all MTSL and BSL samples for are shown in Figures 4 and 5. Figures 4 and 5 clearly indicate that the signal intensity at a particular decay time of 3  $\mu$ s is higher by  $\sim$  3 fold for the lipodisq nanoparticles samples when compared to the proteoliposome samples. All 6 data sets could not be adequately fit with a single exponential decay to directly compare  $T_m$  values for the different samples. However, qualitatively the  $T_m$  values of the lipodisq nanoparticles KCNE1 samples have increased by a factor of  $\sim$ 2 when compared to KCNE1 in proteoliposomes. The S/N of the time domain DEER data for the lipodisq nanoparticles sample is comparable to that for LMPG micelles due to similar  $T_m$  values. A substantial improvement in the information content in the DEER data was achieved by combining the lipodisq nanoparticles sample methodology with the BSL for KCNE1 (see Figure 3C). This data set has the best distance constraints (FWHM of  $\sim$ 6 Å) with the best defined L-curve (see Figure S2C). This is quite significant as researchers have often been confronted with the quandary of sacrificing the biological relevance of the experiment in the interest of data quality when choosing micelle preparations over liposomes.

The DEER data clearly show that comparable signal sensitivity, transverse relaxation time, and accurate and precise distances can be obtained in the more biologically relevant lipodisq nanoparticles when compared to micelles. The time domain data of the more rigid BSL for the lipodisq nanoparticles sample is well defined with obvious periodic oscillations, leading to more accurate and precise distance measurements. Clearly, the BSL coupled with lipodisq



nanoparticles samples have significantly improved the resolution of the distance distributions in Figure 3.

The BSL is constrained to be more localized when compared to the MTSL spin label as seen from the measured distance distributions (FWHM) (see Table 1), which can be used as an alternative spin probe to TOAC.<sup>12</sup> The chemical attachment of BSL to pairs of Cys-SH is easy (similar to the MTSL spin label), while incorporation of TOAC as an unnatural amino acid in expression systems is complicated and challenging. The CW-EPR spectra for the BSL-KCNE1 samples (see Figure S3) are consistent with previously reported EPR data for water-soluble proteins.<sup>12, 31</sup> The EPR spectral lineshape of BSL-KCNE1 is in the rigid limit motion. This indicates proper tethering of BSL to both cysteines. In addition BSL can also be used to monitor the motion of the protein backbone to which it is attached without complications arising from the internal modes of the side-chain.<sup>12</sup> The longer  $T_m$  values can also increase the upper limit of distance measurements for membrane proteins, because the DEER data can be collected out further in time.<sup>12</sup> This has been a serious limitation for DEER measurements on membrane protein samples. The similar probable DEER distances obtained for proteoliposomes and lipodisq nanoparticles in Figures 2 and 3 indicate that there is no significant structural perturbation on the membrane protein due to the utilization of lipodisq nanoparticles. Furthermore, previous studies have indicated that no significant structural and functional perturbations on membrane proteins have occurred due to BSL and lipodisq nanoparticles.<sup>12, 13, 17</sup>

In conclusion, we demonstrated methodological developments in biochemical and spectroscopic techniques to obtain significant improvements in the quality of DEER distance measurements for membrane protein studies. Narrower DEER distance distributions were obtained for BSL when compared to the standard MTSL. The BSL in combination with bacterial overexpression used in this study for KCNE1 indicates that this powerful approach can be utilized for any membrane protein system with no size limitations. The usage of lipodisq nanoparticles improves the quality of distance measurement and experimental throughput by increasing the phase memory time ( $T_m$ ) by a factor of  $\sim 2$  and the S/N by a factor of  $\sim 3$  to 4 when compared to proteoliposomes. The increase in  $T_m$  will allow longer DEER distances to be measured more accurately. Combining these technical improvements (BSL, lipodisq nanoparticles, and pulsed Q-band EPR spectroscopy) for DEER measurements will provide a powerful approach to obtain high quality distance data in a short period of time in order to answer pertinent structural questions for challenging membrane protein systems.

## Supplementary Material

Refer to Web version on PubMed Central for supplementary material.

## Acknowledgments

This work was generously supported by National Institutes of Health Grants R01 GM108026 (to GAL), R01 GM080542 (to GAL), and R01 DC007416 (to CRS). Funding was also provided by National Science Foundation (NSF) Grant CHE-1011909 (to GAL). The pulsed EPR spectrometer was purchased through the NSF and the Ohio Board of Regents grants (MRI-0722403).

## ABBREVIATIONS

<b>SDSL</b>	site-directed spin labeling
<b>CW-EPR</b>	continuous wave electron paramagnetic resonance

<b>PELDOR</b>	pulsed electron double resonance
<b>DEER</b>	double electron-electron resonance
<b>NMR</b>	nuclear magnetic resonance
<b>TMD</b>	transmembrane domain
<b>MSP</b>	membrane scaffold protein
<b>IPTG</b>	isopropyl-1-thio--D-galactopyranoside
<b>SDS-PAGE</b>	sodium dodecyl sulfate polyacrylamide gel electrophoresis
<b>LMPG</b>	1-Myristoyl-2-Hydroxy-sn-Glycero-3-Phospho-(1 -rac-Glycerol) (Sodium Salt)
<b>BSL</b>	bi-functional spin label (3,4-Bis-(methanethiosulfonylmethyl)-2,2,5,5-tetramethyl-2,5-dihydro-1-H-pyrrol-1-yloxy Radical), (HO-1944)
<b>MTSL</b>	1-oxyl-2,2,5,5-tetramethylpyrroline-3-methylmethanethiosulfonate
<b>POPC</b>	1-palmitoyl-2-oleoyl- <i>sn</i> -glycero-3-phosphocholine
<b>POPG</b>	1-palmitoyl-2-oleoyl- <i>sn</i> -glycero-3-phospho (1 - <i>rac</i> -glycerol) (sodium salt)
<b>FWHM</b>	full width of the distribution at half maxima
<b>TOAC</b>	2,2,6,6-tetramethyl-piperidine-1-oxyl-4-amino-4-carboxylic acid.

## REFERENCES

- (1). Borbat PP, Mchaourab HS, Freed JH. Protein structure determination using long-distance constraints from double-quantum coherence ESR: Study of T4 lysozyme. *J. Am. Chem. Soc.* 2002; 124:5304–5314. [PubMed: 11996571]
- (2). Jeschke G, Polyhach Y. Distance measurements on spin-labelled biomacromolecules by pulsed electron paramagnetic resonance. *Phys. Chem. Chem. Phys.* 2007; 9:1895–1910. [PubMed: 17431518]
- (3). Mchaourab HS, Steed PR, Kazmier K. Toward the Fourth Dimension of Membrane Protein Structure: Insight into Dynamics from Spin-Labeling EPR Spectroscopy. *Structure.* 2011; 19:1549–1561. [PubMed: 22078555]
- (4). Jeschke G. DEER Distance Measurements on Proteins. *Annu. Rev. Phys. Chem.* 2012; 63:419–446. [PubMed: 22404592]
- (5). Zou P, Bortolus M, Mchaourab HS. Conformational Cycle of the ABC Transporter MsbA in Liposomes: Detailed Analysis Using Double Electron-Electron Resonance Spectroscopy. *J. Mol. Biol.* 2009; 393:586–597. [PubMed: 19715702]
- (6). Endeward B, Butterwick JA, MacKinnon R, Prisner TF. Pulsed Electron-Electron Double-Resonance Determination of Spin-Label Distances and Orientations on the Tetrameric Potassium Ion Channel KcsA. *J. Am. Chem. Soc.* 2009; 131:15246–15250. [PubMed: 19919160]
- (7). Georgieva ER, Ramlall TF, Borbat PP, Freed JH, Eliezer D. Membrane-bound alpha-synuclein forms an extended helix: Long-distance pulsed ESR measurements using vesicles, bicelles, and rodlike micelles. *J. Am. Chem. Soc.* 2008; 130:12856–12857. [PubMed: 18774805]
- (8). Zou P, Mchaourab HS. Increased Sensitivity and Extended Range of Distance Measurements in Spin-Labeled Membrane Proteins: Q-Band Double Electron-Electron Resonance and Nanoscale Bilayers. *Biophys. J.* 2010; 98:L18–L20. [PubMed: 20303847]
- (9). Xu Q, Ellena JF, Kim M, Cafiso DS. Substrate-dependent unfolding of the energy coupling motif of a membrane transport protein determined by double electron-electron resonance. *Biochemistry.* 2006; 45:10847–10854. [PubMed: 16953570]
- (10). Dastvan R, Bode BE, Karuppiah MPR, Marko A, Lyubenova S, Schwalbe H, Prisner TF. Optimization of Transversal Relaxation of Nitroxides for Pulsed Electron-Electron Double

Resonance Spectroscopy in Phospholipid Membranes. *J. Phys. Chem. B.* 2010; 114:13507–13516. [PubMed: 20923225]

- (11). Hilger D, Polyhach Y, Jung H, Jeschke G. Backbone Structure of Transmembrane Domain IX of the Na<sup>+</sup>/Proline Transporter PutP of *Escherichia coli*. *Biophys. J.* 2009; 96:217–225. [PubMed: 19134477]
- (12). Fleissner MR, Bridges MD, Brooks EK, Cascio D, Kálai T, Hideg K, Hubbell WL. Structure and dynamics of a conformationally constrained nitroxide side chain and applications in EPR spectroscopy. *Proc. Natl. Acad. Sci.* 2011; 108:16241–16246. [PubMed: 21911399]
- (13). Orwick-Rydmark M, Lovett JE, Graziadei A, Lindholm L, Hicks MR, Watts A. Detergent-Free Incorporation of a Seven-Transmembrane Receptor Protein into Nanosized Bilayer Lipodisq Particles for Functional and Biophysical Studies. *Nano Lett.* 2012; 12:4687–4692. [PubMed: 22827450]
- (14). Polyhach Y, Bordignon E, Tschaggelar R, Gandra S, Godt A, Jeschke G. High sensitivity and versatility of the DEER experiment on nitroxide radical pairs at Q-band frequencies. *Phys. Chem. Chem. Phys.* 2012; 14:10762–10773. [PubMed: 22751953]
- (15). Höfer P, Heilig R, Schmalbein D. The superQ-FT accessory for pulsed EPR, ENDOR and ELDOR at 34 GHz. *Bruker Spin Report.* 2003:37–43.
- (16). Ghimire H, McCarrick RM, Budil DE, Lorigan GA. Significantly Improved Sensitivity of Q-Band PELDOR/DEER Experiments Relative to X-Band Is Observed in Measuring the Intercoil Distance of a Leucine Zipper Motif Peptide (GCN4-LZ). *Biochemistry.* 2009; 48:5782–5784. [PubMed: 19476379]
- (17). Orwick MC, Judge PJ, Procek J, Lindholm L, Graziadei A, Engel A, Grobner G, Watts A. Detergent-Free Formation and Physicochemical Characterization of Nanosized Lipid-Polymer Complexes: Lipodisq. *Angew.Chem., Int. Ed.* 2012; 51:4653–4657.
- (18). Kang C, Tian C, Sonnichsen FD, Smith JA, Meiler J, George ALJ, Vanoye CG, Kim HJ, Sanders CR. Structure of KCNE1 and Implications for How It Modulates the KCNQ1 Potassium Channel. *Biochemistry.* 2008; 47:7999–8006. [PubMed: 18611041]
- (19). Tian C, Vanoye CG, Kang C, Welch RC, Kim HJ, George AL, Sanders CR. Preparation, Functional Characterization, and NMR Studies of Human KCNE1, a Voltage-Gated Potassium Channel Accessory Subunit Associated with Deafness and Long QT Syndrome. *Biochemistry.* 2007; 46:11459–11472. [PubMed: 17892302]
- (20). Coey AT, Sahu ID, Gunasekera TS, Troxel KR, Hawn JM, Swartz MS, Wickenheiser MR, Reid R. -j, Welch RC, Vanoye CG, Kang C, Sanders CR, Lorigan GA. Reconstitution of KCNE1 into Lipid Bilayers: Comparing the Structural, Dynamic, and Activity Differences in Micelle and Vesicle Environments. *Biochemistry.* 2011; 50:10851–10859. [PubMed: 22085289]
- (21). Melman YF, Um SY, Krumerman A, Kagan A, McDonald TV. KCNE1 binds to the KCNQ1 pore to regulate potassium channel activity. *Neuron.* 2004; 42:927–937. [PubMed: 15207237]
- (22). Panaghie G, Tai KK, Abbott GW. Interaction of KCNE subunits with the KCNQ1 K<sup>+</sup> channel pore. *J. Physiol.* 2006; 570:455–467. [PubMed: 16308347]
- (23). Li G-R, Feng J, Yue L, Carrier M, Nattel S. Evidence for two components of delayed rectifier K<sup>+</sup> current in human ventricular myocytes. *Circ. Res.* 1996; 78:689–696. [PubMed: 8635226]
- (24). Jost N, Virag L, Bitay M, Takacs J, Lengye I, C. Biliczki P, Nagy Z, Bogats G, Lathrop DA, Papp JG, Varro A. Restricting excessive cardiac action potential and QT prolongation. A vital role for I<sub>Ks</sub> in human ventricular muscle. *Circulation.* 2005; 112:1392–1399. [PubMed: 16129791]
- (25). Wang Z, Fermini B, Nattel S. Rapid and slow components of delayed rectifier current in human atrial myocytes. *Cardiovasc. Res.* 1994; 28:1540–1546. [PubMed: 8001043]
- (26). Harmer SC, Tinker A. The role of abnormal trafficking of KCNE1 in long QT syndrome 5. *Biochem. Soc. Trans.* 2007; 35:1074–1076. [PubMed: 17956282]
- (27). Barrett PJ, Song Y, Van Horn WD, Hustedt EJ, Schafer JM, Hadziselimovic A, Beel AJ, Sanders CR. The Amyloid Precursor Protein Has a Flexible Transmembrane Domain and Binds Cholesterol. *Science.* 2012; 336:1168–1171. [PubMed: 22654059]
- (28). Feldmann EA, Ni S, Sahu ID, Mishler CH, Risser DD, Murakami JL, Tom SK, McCarrick RM, Lorigan GA, Tolbert BS, Callahan SM, Kennedy MA. Evidence for Direct Binding between



HetR from *Anabaena* sp PCC 7120 and PatS-5. *Biochemistry*. 2011; 50:9212–9224. [PubMed: 21942265]

- (29). Jeschke G, Chechik V, Ionita P, Godt A, Zimmermann H, Banham J, Timmel CR, Hilger D, Jung H. DeerAnalysis2006 - a comprehensive software package for analyzing pulsed ELDOR data. *Appl. Magn. Reson.* 2006; 30:473–498.
- (30). Chiang YW, Borbat PP, Freed JH. The determination of pair distance distributions by pulsed ESR using Tikhonov regularization. *J. Mag. Reson.* 2005; 172:279–295.
- (31). Moen RJ, Thomas DD, Klein JC. Conformationally Trapping the Actin-binding Cleft of Myosin with a Bifunctional Spin Label. *J. Biol. Chem.* 2013; 288:3016–3024. [PubMed: 23250750]

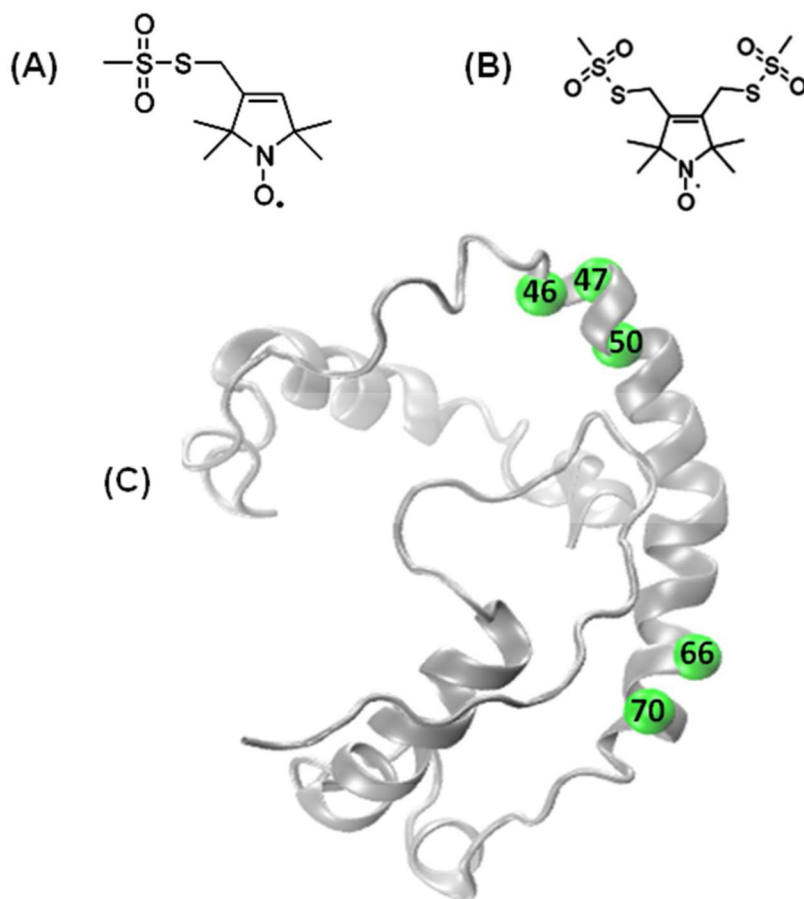


**Figure 1.** Schematic representation of spin labeling probes and sites: (A) MTSL and (B) BSL, and (C) Ribbon model of KCNE1 (PDB ID: 2k21) highlighting representative sites used in this study with spheres at their  $\alpha$  carbons. All spin labeling sites are located inside the membrane. The spin labeling sites 46 and 70 on KCNE1 are near the ends of the transmembrane domain (45-71) that spans the membrane bilayer.

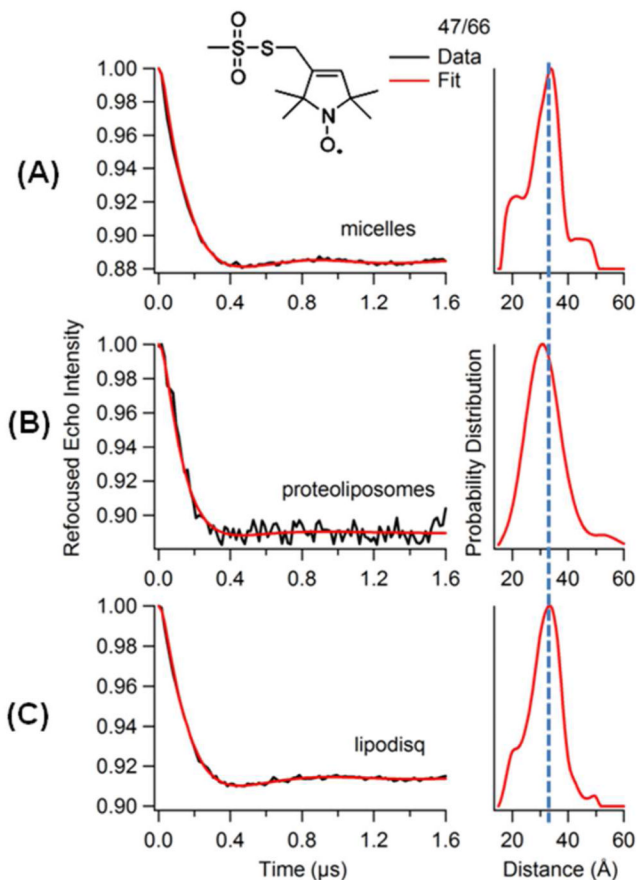


**Figure 2.** Q-band DEER data of E1 mutants (Val47/Ile66) bearing two MTSL spin labels. Background-subtracted dipolar evolutions of the indicated mutants (left) and their corresponding distance probability distributions from Tikhonov regularization (right) for 1 % LMPG micelles (A) proteoliposomes (POPC/POPG=3:1) (B), and lipodisq nanoparticles (C).

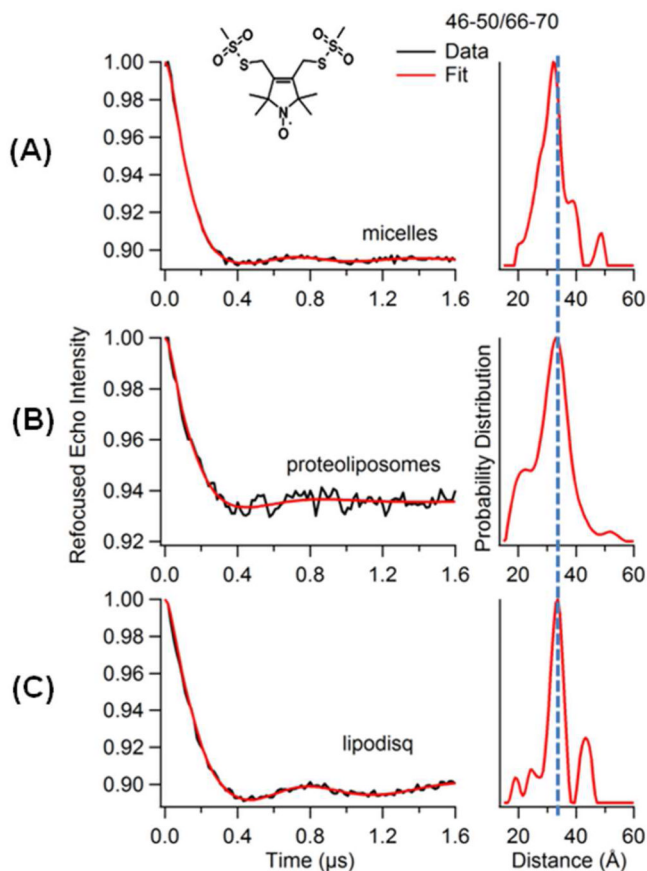


**Figure 3.** Q-band DEER data of E1 mutants (Tyr46-Val50/Ile66-Lys70) bearing two BSLs. Background-subtracted dipolar evolutions of the indicated mutants (left) and their corresponding distance probability distributions from Tikhonov regularization (right) for 1% LMPG micelles (A), proteoliposomes (POPC/POPG=3:1) (B), and lipodisq nanoparticles (C).

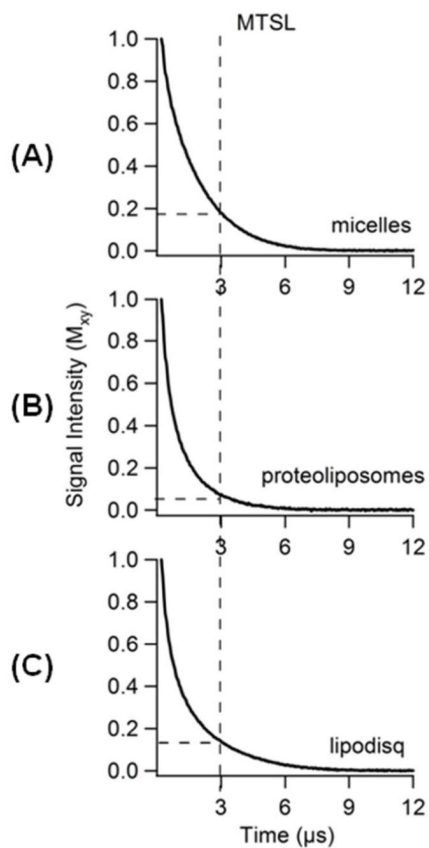


**Figure 4.** Experimental phase memory curves for dual spin labeled E1 mutants (Val47/Ile66) bearing two MTSL spin labels for 1% LMPG micelles ( $T_m = 1.9 \pm 0.2 \mu\text{s}$ ) (A) POPC/POPG=3:1 proteoliposomes ( $T_m = 1.0 \pm 0.2 \mu\text{s}$ ) (B), and lipodisq nanoparticles ( $T_m = 1.9 \pm 0.2 \mu\text{s}$ ) (C).



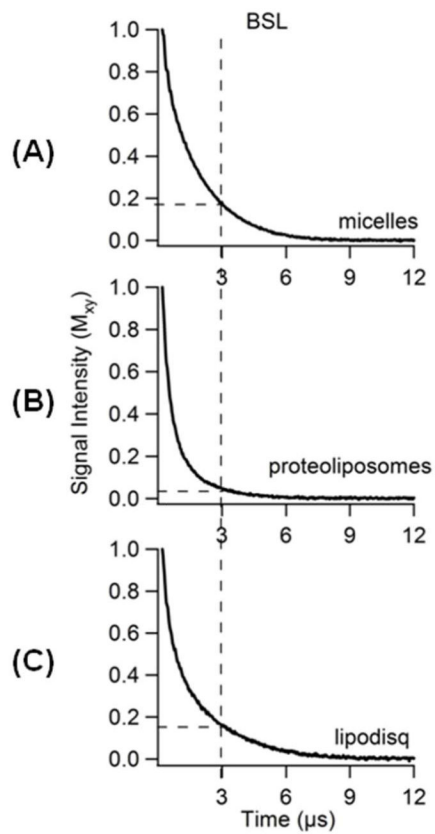


**Figure 5.**

Experimental phase memory curves for dual spin labeled E1 mutants (Tyr46-Val50/Ile66-Lys70) bearing two BSLs for 1% LMPG micelles ( $T_m = 1.9 \pm 0.2 \mu\text{s}$ ) (A) POPC/POPG=3:1 proteoliposomes ( $T_m = 0.9 \pm 0.2 \mu\text{s}$ ) (B), and lipodisq nanoparticles ( $T_m = 1.9 \pm 0.2 \mu\text{s}$ ) (C).

**Table 1**

The approximate full width of the distribution at half maxima (FWHM) from DEER distance measurements on the KCNE1 membrane protein.

KCNE1 Double Mutants	Micelles FWHM (Å)	Liposomes FWHM (Å)	Lipodisq FWHM (Å)
47/66 (MTSL)	~12	~17	~12
46-50/66-70 (BSL)	~8	~11	~6